British Journal of Pharmacology

DOI:10.1111/j.1476-5381.2010.01104.x
www.brjpharmacol.org

RESEARCH PAPER

Characterization of the metabolism of fenretinide by human liver microsomes, cytochrome P450 enzymes and UDP-glucuronosyltransferases

NA Illingworth[1], AV Boddy[1], AK Daly[2] and GJ Veal[1]

[1]*Northern Institute for Cancer Research and* [2]*Institute of Cellular Medicine, Newcastle University, Newcastle upon Tyne, UK*

Correspondence
Dr Gareth J. Veal, Northern Institute for Cancer Research, Paul O'Gorman Building, Medical School, Framlington Place, University of Newcastle upon Tyne, Newcastle upon Tyne NE2 4HH, UK. E-mail: G.J.Veal@ncl.ac.uk

Keywords
fenretinide; metabolism; microsomes; cytochrome P450; CYP2C8; UDP-glucuronosyltransferases

Received
21 July 2010
Revised
16 September 2010
Accepted
12 October 2010

BACKGROUND AND PURPOSE
Fenretinide (4-HPR) is a retinoic acid analogue, currently used in clinical trials in oncology. Metabolism of 4-HPR is of particular interest due to production of the active metabolite 4'-oxo 4-HPR and the clinical challenge of obtaining consistent 4-HPR plasma concentrations in patients. Here, we assessed the enzymes involved in various 4-HPR metabolic pathways.

EXPERIMENTAL APPROACH
Enzymes involved in 4-HPR metabolism were characterized using human liver microsomes (HLM), supersomes over-expressing individual human cytochrome P450s (CYPs), uridine 5'-diphospho-glucoronosyl transferases (UGTs) and CYP2C8 variants expressed in *Escherichia coli*. Samples were analysed by high-performance liquid chromatography and liquid chromatography/mass spectrometry assays and kinetic parameters for metabolite formation determined. Incubations were also carried out with inhibitors of CYPs and methylation enzymes.

KEY RESULTS
HLM were found to predominantly produce 4'-oxo 4-HPR, with an additional polar metabolite, 4'-hydroxy 4-HPR (4'-OH 4-HPR), produced by individual CYPs. CYPs 2C8, 3A4 and 3A5 were found to metabolize 4-HPR, with metabolite formation prevented by inhibitors of CYP3A4 and CYP2C8. Differences in metabolism to 4'-OH 4-HPR were observed with 2C8 variants, CYP2C8*4 exhibited a significantly lower V_{max} value compared with *1. Conversely, a significantly higher V_{max} value for CYP2C8*4 versus *1 was observed in terms of 4'-oxo formation. In terms of 4-HPR glucuronidation, UGTs 1A1, 1A3 and 1A6 produced the 4-HPR glucuronide metabolite.

CONCLUSIONS AND IMPLICATIONS
The enzymes involved in 4-HPR metabolism have been characterized. The CYP2C8 isoform was found to have a significant effect on oxidative metabolism and may be of clinical relevance.

Abbreviations
13-cisRA, 13-cis retinoic acid; 4-HPR, fenretinide; 4-MPR, 4-methoxy fenretinide; ATRA, all-trans retinoic acid; COMT, catechol-O-methyltransferases; CYP, cytochrome P450; HIM, human intestinal microsomes; HLM, human liver microsomes; PMT, phenol methyltransferase; SAM, S-adenosyl methionine; UGT, uridine 5'-diphospho-glucoronosyl transferases

Introduction

Fenretinide (4-HPR) is a synthetic analogue of retinoic acid, currently used in clinical trials in children for the treatment of neuroblastoma. In addition, Ewing's sarcoma cell lines have been shown to be sensitive to 4-HPR treatment *in vitro* (Lovat *et al.*, 2000; Myatt and Burchill, 2007) and 4-HPR has been shown to be effective in pre-clinical animal studies (Ponthan *et al.*, 2003; Maurer *et al.*, 2007). As both of these paediatric cancers have 5-year survival rates of less than 60% (Gatta *et al.*, 2002), improvements in their clinical treatment are clearly needed. Unlike other retinoid derivatives currently in use in the clinic, such as all-*trans* retinoic acid (ATRA) and 13-*cis* retinoic acid (13-cisRA), 4-HPR induces apoptosis as well as differentiation (Kitareewan *et al.*, 1999), and is also better tolerated than other retinoids (Garaventa *et al.*, 2003). The metabolism of both ATRA and 13-cisRA have previously been characterized, with cytochrome P450 enzymes (CYPs) including 2C8, 3A7, 3A5, 2C18, 3A4 and 2C9 having been identified in the metabolism of ATRA, and CYPs including 2C8, 3A7, 4A11, 1B1, 2B6 and 2C9 responsible for the metabolism of 13-cisRA (Marill *et al.*, 2000; 2002; McSorley and Daly, 2000). While 4-HPR metabolism is similar to that of ATRA and 13-*cis* retinoic acid in many respects, 4-HPR produces an active metabolite, 4′-oxo fenretinide (4′-oxo 4-HPR), which is able to act synergistically with 4-HPR and is also active against some 4-HPR-resistant cell lines (Villani *et al.*, 2006). 4-HPR is also metabolized to an inactive metabolite in the form of 4-methoxy fenretinide (4-MPR) (Mehta *et al.*, 1998), with significant metabolism to both of these metabolites observed in clinical trials (Villani *et al.*, 2004; Villablanca *et al.*, 2006; Formelli *et al.*, 2008). Although the formation of glucuronide metabolites of fenretinide has not previously been reported, this metabolic pathway may be applicable to fenretinide as glucuronidation of other retinoids has been described by our group and others (Czernik *et al.*, 2000; Samokyszyn *et al.*, 2000; Rowbotham *et al.*, 2010a). As one of the main limitations to the clinical development of orally administered 4-HPR is the achievement of effective and consistent plasma concentrations in patients (Maurer *et al.*, 2007), metabolism of the parent drug is clearly an important issue. The aim of the current study was to characterize the *in vitro* metabolism of 4-HPR in human liver microsomes (HLM), supersomes overexpressing individual human CYPs, CYP2C8 variants expressed in *Escherichia coli* and a panel of recombinant human uridine 5′-diphospho-glucoronosyl transferases (UGTs).

Methods

Chemicals

CYP2C8 clones were kindly provided by Dr Frank J Gonzalez of the National Cancer Institute, Bethesda, MD, USA. The human P450 reductase clone was kindly provided by Dr Thomas Friedberg of the University of Dundee. 4-HPR and 4-MPR were generously provided by Cancer Research UK and 4′-oxo-4-HPR was provided by High Force Research Ltd. (Durham, UK). Anti-CYP reductase, anti-CYP 2C8 and horseradish peroxidase-linked donkey anti-rabbit IgG antibodies were purchased from Millipore (Watford, UK). HLM, HIM, CYP supersomes and UGT supersomes were supplied by BD Biosciences (Oxford, UK). Bactopeptone, bactotryptone, yeast extract and bactoagar were purchased from Difco Laboratories (East Mosely, UK). ECL Plus Western blotting detection reagents were obtained from G E Healthcare (Buckinghamshire, UK). Tris-glycine gels were supplied by Invitrogen (Paisley, UK). JM109 competent cells were purchased from Promega (Southampton, UK). Carbon monoxide was supplied by BOC gases (Guildford, UK). high-performance liquid chromatography (HPLC)-grade solvents were from Fisher Scientific (Loughborough, UK). All other chemicals and reagents were purchased from Sigma-Aldrich (Poole, UK).

Liquid chromatography/mass spectrometry (LC/MS) analysis of 4-HPR and metabolites

Separation of 4-HPR and its metabolites was achieved using a Perkin Elmer LC (Beaconsfield, UK) system, consisting of a vacuum degasser, two series 200 pumps, a thermostatically controlled series 200 autosampler and a Waters 2487 UV absorbance detector. Reverse-phase chromatography was performed using a Luna 3 µm C18 50 × 2 mm column with a flow rate of 250 µL·min^{-1} and an injection volume of 10 µL. Mobile phases consisted of (A) 40% acetonitrile/60% (0.2%) acetic acid and (B) acetonitrile/0.2% acetic acid. A linear gradient ran from 100% A at 0 min to 100% B at 3 min, at which it was maintained for 2.5 min before returning to 100% A. An Applied Biosystems (Warrington, UK) API-2000 liquid chromatography/mass spectrometry/mass spectrometry (LC/MS/MS) triple Q (quadrupole) mass spectrometer with electrospray ionization source, controlled by Analyst software, was operated in single quadrupole negative mode for the detection of 4-HPR [multiple reaction monitoring (MRM) of 392/283], 4′-hydroxy 4-HPR (4′OH 4-HPR) (MRM 407/299) and 4′-oxo 4-HPR (MRM 406/297).

HPLC analysis of 4-HPR and metabolites

HPLC analysis was carried out using a Waters 2690 Separations Module and 996 photodiode array (PDA) detector (Waters Ltd, Elstree, UK), with Waters Millennium software for data acquisition, based on the previously published method of Formelli *et al.* (1993). Separation of 4-HPR, 4′-OH 4-HPR, 4′-oxo 4-HPR and 4-MPR was achieved using a Waters Symmetry C18 3.5 µm (4.6 × 150 mm) column, with mobile phases (A) 70% acetonitrile/30% (0.2%) acetic acid and (B) acetonitrile/0.2% acetic acid. A linear gradient ran at 1 mL·min^{-1} from 100% A at 0 min to 100% B at 20 min, returning to 100% A for 10 min to re-equilibrate the column. A sample volume of 50 µL was injected onto the column for analysis. Separation of 4-HPR and its glucuronide metabolites was achieved using a Luna C18 (2) column (50 × 2.0 mm, 3 µm) (Phenomenex, Torrance, CA, USA), was used with mobile phases (A) 0.1% acetic acid, pH 5.0 and (B) 100% acetonitrile. A linear gradient ran at 0.2 mL·min^{-1} from 60% A at 0 min to 100% B at 6 min, maintaining at 100% B for 4 min and returning to 60% A for 10 min to re-equilibrate the column. A sample volume of 20 µL was injected onto the column for analysis. The limit of quantification of the assay was 0.01 µg·mL^{-1} and the inter-assay coefficients of variation were 4.3–6.5% for 4-HPR and metabolites.

Incubation of 4-HPR with HLM, HIM, CYP supersomes and UGT supersomes

HLM or a panel of CYP supersomes (up to 1 mg·mL^{-1} protein) over-expressing individual human CYPs were incubated with 50 μM 4-HPR in 0.1 M phosphate buffer, pH 7.4, containing 1 mM $MgCl_2$ and 2 mM nicotinamide adenine dinucleotide phosphate in a final volume of 200 μL for 3 h. CYPs 1A6, 2B6, 2E1, 3A4, 3A5, 2C8, 2C9 and 2C19 were used. For experiments investigating 4-HPR glucuronidation, HLM, HIM or a panel of UGT supersomes over-expressing individual UGTs were incubated with 200 μM 4-HPR in an incubation mixture consisting of alamethecin (25 μg·mL^{-1}), $MgCl_2$ (8 mM), uridine diphosphate glucuronic acid (2 mM) and methanol (0.25%), made up to a final volume (50 μL) with Tris-HCl buffer (50 mM, pH 7.5). UGTs 1A1, 1A3, 1A4, 1A6, 1A7, 1A8, 1A9, 1A10, 2B4, 2B5, 2B15 and 2B17 were used. Incubations were carried out at 37°C for 3 h. Reactions were initiated by the addition of enzyme and terminated with ice-cold acetonitrile (100 μL). To confirm that the metabolite produced was a glucuronide, β-glucuronidase (800 U) in potassium phosphate buffer (75 mM, pH 6.8) was added to samples prepared from the incubations as described above, and the mixture was incubated at 37°C for 30 min. All reactions were terminated by the addition of ice-cold acetonitrile (400 μL) and samples were centrifuged at 10 000× *g* for 5 min to remove all protein. Supernatant was then retained for HPLC analysis. Experiments were carried out in parallel, with all comparative samples for a defined experiment being analysed within a single assay.

Determination of kinetic parameters for 4′-OH 4-HPR, 4′-oxo 4-HPR, 4-MPR and 4-HPR glucuronide formation

Kinetic parameters for the formation of 4′-OH 4-HPR, 4′-oxo 4-HPR and 4-MPR were determined following incubations of 0–1 mg·mL^{-1} protein of HLM or CYP3A4, 3A5 or 2C8 supersomes with 50 μM 4-HPR, or 0–100 μM 4-HPR with 0.25 mg·mL^{-1} protein. Incubations to determine 4-MPR formation also had 0.2 mM S-adenosyl methionine (SAM) added as a methylation co-factor. Kinetic parameters for the formation of the glucuronide metabolite of 4-HPR were determined following incubations of 0–1.5 mg·mL^{-1} protein of HLM, HIM or UGTs 1A1, 1A3 or 1A6 with 200 μM 4-HPR, or 0–2 mM 4-HPR with 1 mg·mL^{-1} protein. Calculations were performed with GraphPad Prism version 4.0 software (GraphPad Software Inc., San Diego, CA, USA). Because of the lack of authentic standards for 4′-OH 4-HPR and 4-HPR glucuronide, V_{max} results were calculated in peak area U·min^{-1}.

Determination of kinetic parameters for 4′-OH 4-HPR and 4′-oxo 4-HPR formation by CYP2C8 variants

JM109 high competency *E. coli* cells were transfected with plasmids for CYP variants *1 (wild type), *3, *4 or an empty plasmid (control), and co-transfected with CYP reductase prior to the generation of membrane fractions as previously described (Rowbotham *et al.*, 2010b). The level of CYP2C8 and P450 reductase expression was assessed by sodium dodecyl sulphate-polyacrylamide gel electrophoresis on 4–20% tris-glycine gels followed by Western blotting with rabbit anti-CYP2C8 and rabbit anti-P450 reductase antibody, followed by horseradish peroxidase-linked donkey anti-rabbit IgG secondary antibody. Detection was by enhanced chemiluminescence. CYP content was measured using Fe^{2+}-CO versus Fe^{2+} difference spectra and P450 reductase content was measured using the cytochrome C reductase assay as previously described (Rowbotham *et al.*, 2010b).

Kinetic parameters for the formation of 4′-OH 4-HPR and 4′-oxo 4-HPR were determined following incubations of 0–1 mg·mL^{-1} protein of CYP2C8 isoform membrane fractions with 50 μM 4-HPR, or 0–100 μM 4-HPR with 0.25 mg·mL^{-1} protein. Because of the lack of an authentic standard for 4′-OH 4-HPR, V_{max} results are given in peak area U·min^{-1}. One-way analysis of variance was used to compare K_m and V_{max} data, with $P < 0.05$ used to determine significance. Individual CYP2C8 variants were then compared with wild type by use of Student's *t*-test. All calculations were performed with GraphPad Prism version 4.0 software (GraphPad Software Inc.).

Inhibition of 4-MPR

Known inhibitors or competitive substrates of several methylating enzymes were added to HLM incubations. Compounds used were: 4-nitrocatechol, nialamide, pargyline [inhibitors of catechol-O-methyltransferases (COMT)], acetaminophen [inhibitor of phenol methyltransferase (PMT)] and imidazole (competitive substrate for amino-N-methyltransferase). HLM (0.5 mg·mL^{-1}) were incubated with 50 μM 4-HPR, 0.2 mM SAM and 0–5 mM inhibitor in 0.1 M phosphate buffer, pH 7.4, containing 1 mM $MgCl_2$ and 2 mM NADPH in a final volume of 200 μL for 3 h. The reaction was stopped by addition of 400 μL acetonitrile, and samples were centrifuged at 10 000× *g* for 5 min to remove all protein. Supernatant was then retained for HPLC analysis.

Results

Chromatographic analysis of 4-HPR and its metabolites

Following incubation of 4-HPR with HLM, the metabolites produced were analysed by LC/MS/MS and HPLC. Peaks were identified for 4-HPR and its two main polar metabolites, 4′OH-4-HPR and 4′-oxo 4-HPR, in addition to 4-HPR glucuronide, as shown in Figure 1. 4-HPR and 4′-oxo 4-HPR were identified by co-elution with authentic standards and by their mass spectrometry/mass spectrometry (MS/MS) profiles. 4′-OH 4-HPR was identified by its MS/MS profile alone and 4-HPR glucuronide was identified by peak removal following incubation of samples with β-glucuronidase, as no authentic standards were available for either of these metabolites. Retention times (RT) for the HPLC assay were 3.5 min, 3.9 min and 13.5 min for 4′-OH 4-HPR, 4′-oxo 4-HPR and 4-HPR respectively. RT for the HPLC assay used for identification of 4-HPR glucuronide were 6.9 min for 4-HPR glucuronide and 11.1 min for 4-HPR. Additional peaks seen at similar RT to 4-HPR were isomers of 4-HPR. LC/MS/MS analysis identified 4-HPR with an MRM of 392/283 (RT 5. 8 min), 4′-OH 4-HPR with an MRM of 407/299 (RT 4.3 min), and 4′-oxo 4-HPR with an MRM of 406/297 (RT 5.1 min).

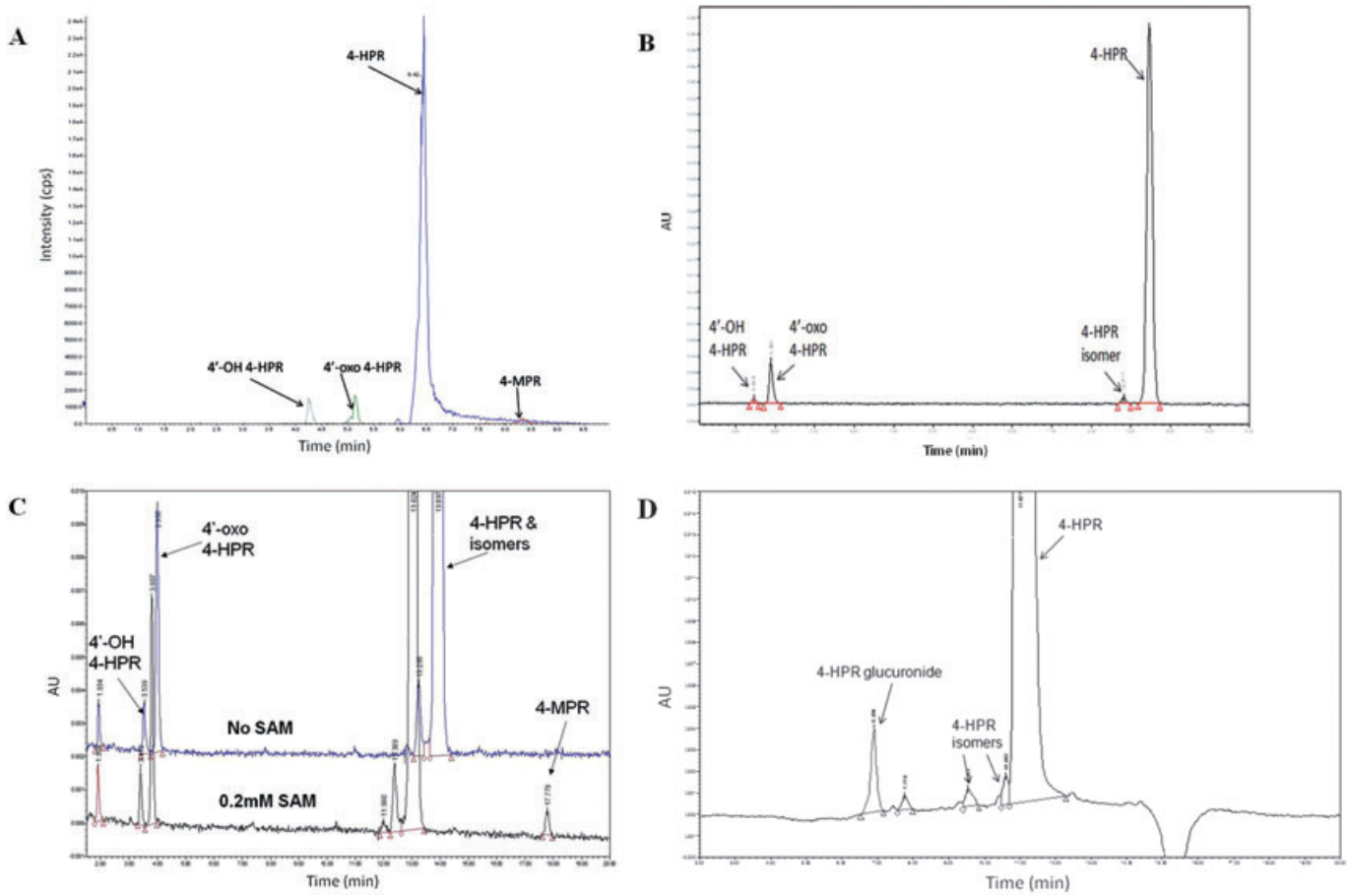

Figure 1

Representative chromatograms showing separation of fenretinide (4-HPR) and metabolites by LC/MS/MS (A) and reversed-phase high-performance liquid chromatography (B, C and D). Metabolites were generated following a 3-h incubation of 20 μM 4-HPR with 0.5 mg·mL^{-1} human liver microsomes (HLM; A, B and C) or following a 3-h incubation of 200 μM 4-HPR with 0.5 mg·mL^{-1} HLM (D). Generation of methoxy fenretinide (4-MPR) is shown in (C) in the presence of 0.2 mM S-adenosyl methionine (SAM).

Incubation of 4-HPR with CYP supersomes

4-HPR 50 μM was incubated with a panel of supersomes over-expressing individual human CYPs, to identify the enzymes responsible for the oxidation and hydroxylation of 4-HPR. While all CYPs tested were able to generate 4′-OH 4-HPR, as shown in Figure 2, CYPs 3A4, 3A5 and 2C8 clearly produced the highest levels. Only CYPs 3A4 and 2C8 were able to generate 4′-oxo 4-HPR, the known active metabolite of 4-HPR.

Determination of kinetic parameters for 4′-OH 4-HPR, 4′-oxo 4-HPR and 4-MPR formation

4-HPR was incubated with HLM or supersomes over-expressing individual human CYPs to determine enzyme kinetic parameters. CYPs 3A4, 3A5 and 2C8 were used, as these had been shown to metabolize 4-HPR to 4′-OH 4-HPR and 4′-oxo 4-HPR. Metabolite production was related to 4-HPR concentration as shown in Figure 3, with kinetic parameters for all three CYPs and HLM presented in Table 1. HLM were the most effective at metabolizing 4-HPR to the known active metabolite 4′-oxo 4-HPR, with a V_{max} of 131 peak area U·min^{-1}, as compared with V_{max} values of 30, 25 and 0 peak area U·min^{-1} for of the individual CYPs 2C8, 3A4 and 3A5 respectively. In terms of 4′-OH 4-HPR production, HLM exhibited a V_{max} of 28 peak area U·min^{-1}, as compared with V_{max} values of 115–282 peak area U·min^{-1} for supersomes expressing individual CYPs. Results expressed as values normalized for CYP content are also shown for the individual human CYPs in Table 1. Significant differences were observed in V_{max} values between CYP2C8 and CYP3A4 for both 4′-oxo and 4′-OH metabolite formation ($P = 0.0001$ and $P = 0.0005$, respectively) and between CYP2C8 and CYP3A5 for 4′-OH formation ($P < 0.0001$). Because of the level of metabolism seen with CYP2C8, and as 2C8 is known to be polymorphic, the effect of CYP2C8 variants on metabolism was then investigated.

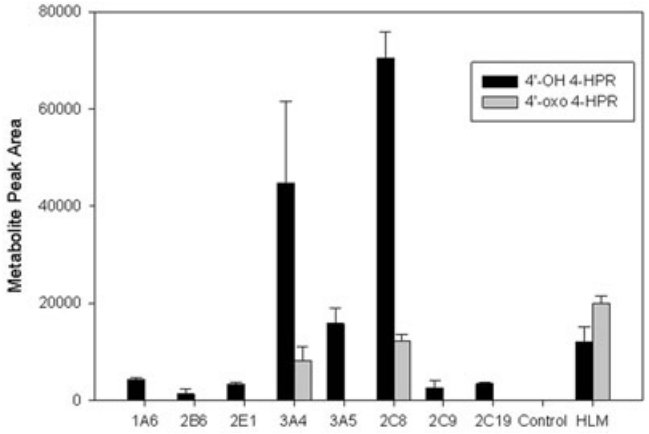

Figure 2

Formation of 4′-OH 4-HPR and 4′-oxo fenretinide (4′-oxo 4-HPR) metabolites of 4-HPR by a panel of supersomes over-expressing individual human cytochrome P450s. Metabolite formation was determined by high-performance liquid chromatography analysis. Control supersomes were from cells transfected with an empty vector. Metabolites were generated by 3-h incubation of 50 μM 4-HPR with 1 mg·mL^{-1} of each supersome for 3 h. Results are mean ± SD from three independent experiments. HLM, human liver microsomes.

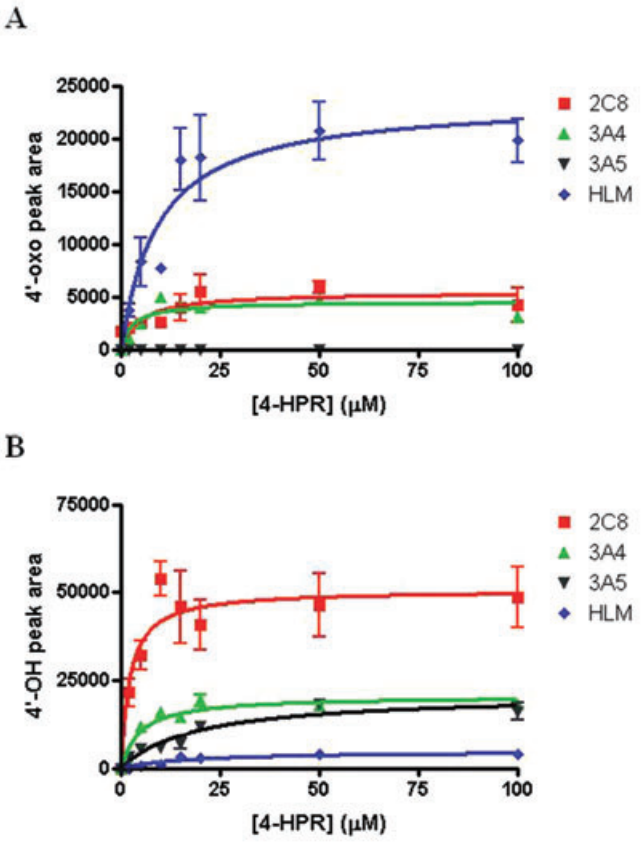

Figure 3

Determination of kinetic parameters for the formation of (A) 4′-oxo fenretinide (4′-oxo 4-HPR) and (B) 4′-OH 4-HPR metabolites by a panel of supersomes over-expressing individual human CYPs. The major CYPs (0.5 mg mL^{-1}) found to metabolize 4-HPR (human cytochrome P450s 3A4, 3A5 and 2C8) were incubated with 0, 2.5, 5, 10, 15, 20, 50 and 100 μM 4-HPR for 3 h. Metabolite formation was determined by high-performance liquid chromatography analysis. Results are mean ± SD from three independent experiments.

Determination of kinetic parameters for 4′-OH 4-HPR and 4′-oxo 4-HPR formation by CYP2C8 variants

The CYP content of *E. coli* transfectants varied from 175–295 pmol·mg^{-1} of protein, and was comparable to CYP2C8 supersomes, which contained 293 pmol of CYP mg^{-1} protein. CYP reductase concentrations ranged from 180–213 nmol·mg^{-1}·min^{-1}, again comparable to CYP2C8 supersomes (176 nmol·mg^{-1}·min^{-1}). 4-HPR was incubated with each CYP2C8 variant to determine enzymatic kinetic parameters. Metabolite production with increasing 4-HPR concentration is shown in Figure 4, with kinetic parameters provided in Table 2. Differences in metabolism to 4′-OH 4-HPR and 4-oxo 4-HPR were observed with the 2C8 variants, most notably with CYP2C8*4. In terms of 4′-OH 4-HPR production, although there were no significant differences in K_m values for *1, *3 and *4 (5.6, 8.6 and 4.3 μM, respectively), V_{max} values for *3 (0.24 peak area U·min^{-1}·pmol^{-1} CYP) and *4 (0.11 peak area U·min^{-1}·pmol^{-1} CYP) were significantly different from *1, which had a V_{max} of 0.20 peak area U·min^{-1}·pmol^{-1} CYP (P = 0.03 and 0.0025 respectively). V_{max}/K_m ratios for 4′-OH 4-HPR were 0.028 and 0.026 for *3 and *4, respectively, as compared with 0.036 for *1. Formation of 4′-oxo 4-HPR by CYP2C8 *1 was characterized by a V_{max} of 0.04 peak area U·min^{-1}·pmol^{-1} CYP and a K_m of 19.3 μM. These results were comparable to V_{max} and K_m values of 0.05 and 18.8 μM, respectively, for CYP2C8*3. However, for CYP2C8*4, the V_{max} was 0.128 peak area U·min^{-1}·pmol^{-1} CYP, and the K_m was 59.8 μM, significantly different from CYP2C8 *1 (P = 0.004).

CYP inhibition

4-HPR was incubated with HLM and CYP inhibitors omeprazole (inhibitor of CYP2C8 and 2C9) and ketoconazole (inhibitor of CYP3A4), either alone or in combination (data not shown). Ketoconazole (100 μM) considerably inhibited the production of both metabolites, with 75% inhibition of 4′-OH 4-HPR and 85% inhibition of 4′-oxo 4-HPR. Omeprazole alone at a concentration of 100 μM had very little effect on the production of either metabolite, but in combination with 100 μM ketoconazole resulted in complete inhibition of the production of both metabolites.

Production of 4-MPR from HLM

Addition of the methylation co-factor SAM to incubations of HLM and 4-HPR resulted in production of 4-MPR (Figure 1C), with 4-MPR peak area increasing with increasing SAM concentrations up to 0.2 mM. This concentration of SAM was added to all microsomal reactions investigating the production of 4-MPR. Figure 5A shows the extent of formation of 4-MPR following incubations of 4-HPR at concentrations of 0–100 μM. A K_m value of 236 μM was determined for 4-MPR formation, markedly higher than those observed for 4′-OH

Table 1

Determination of kinetic parameters for the formation of the 4′-OH 4-HPR and 4′-oxo 4-HPR metabolites of 4-HPR by a panel of supersomes over-expressing individual human CYPs and HLM

	4′-oxo 4-HPR			4′-OH 4-HPR		
	K_m (μM)	V_{max} (peak area U·min^{-1})	(peak area U·min^{-1}·pmol^{-1} CYP)	K_m (μM)	V_{max} (peak area U·min^{-1})	(peak area U·min^{-1}·pmol^{-1} CYP)
HLM	9.3 ± 3.2	131 ± 14	N/A	17.8 ± 9.4	28 ± 6	N/A
3A4	2.8 ± 1.1	25 ± 2	0.43 ± 0.03	4.8 ± 1.2	115 ± 7	2.05 ± 0.1
3A5	N/D	N/D	N/D	19.1 ± 5.0	118 ± 6	1.84 ± 0.1
2C8	5.0 ± 3.1	30 ± 5	0.18 ± 0.03	2.2 ± 1.1	282 ± 24	1.45 ± 0.1

The major CYPs found to metabolize 4-HPR (CYPs 3A4, 3A5 and 2C8) were incubated with 0, 2.5, 5, 10, 15 and 20 μM 4-HPR for 3 h. Metabolite formation was determined by HPLC analysis. Results are expressed as mean ± SD from $n \geq 3$ experiments. V_{max} for 4′-oxo 4-HPR significantly different for CYP3A4 and CYP2C8 ($P = 0.0001$); V_{max} for 4′-OH 4-HPR significantly different for CYP3A4 and CYP2C8 ($P = 0.0005$) and for CYP3A5 and CYP2C8 ($P < 0.0001$); K_m for 4′-OH 4-HPR significantly different for CYP3A4 and CYP3A5 ($P = 0.0085$) and for CYP3A5 and CYP2C8 ($P = 0.0046$). Statistical analysis carried out on supersome data only, with V_{max} results standardized to pmol CYP used for analysis. 4-HPR, fenretinide; 4′-OH 4-HPR, 4′-hydroxy fenretinide; 4′-oxo 4-HPR, 4′-oxo fenretinide; CYP, cytochrome P450; HIM, human intestinal microsomes; HLM, human liver microsomes; N/A, no data available; N/D, not detected.

and 4′-oxo 4-HPR. Similarly, a calculated V_{max} value of 823 peak U·min^{-1} for 4-MPR was higher than those observed for the 4′-OH and 4′-oxo metabolites.

Inhibition of 4-MPR formation

Known inhibitors or competitive substrates of several methylating enzymes were added to HLM incubations. Although inhibitors of COMT and PMT had no effect on 4-MPR production, imidazole (a competitive substrate for amine-N-methyltransferase) inhibited 80% of 4-MPR production, but only at a concentration of 5 mM, as shown in Figure 5B.

Incubation of 4-HPR with UGT supersomes

4-HPR (200 μM) was incubated with a panel of supersomes expressing individual UGT enzymes, as well as HIM and HLM, to identify the enzymes responsible for the production of the glucuronide metabolite of 4-HPR (Figure 1D). Of the UGTs included in the screen, only UGTs 1A1, 1A3 and 1A6, in addition to HIM and HLM, produced 4-HPR glucuronide (Figure 6). Incubation of samples with β-glucuronidase resulted in complete removal of the metabolite peak, confirming it as a glucuronide.

Determination of kinetic parameters for formation of 4-HPR glucuronide

4-HPR was incubated with HLM, HIM or individual UGT enzymes to determine enzyme kinetic parameters. UGTs 1A1, 1A3 and 1A6 were used, as these had been shown to metabolize 4-HPR to its glucuronide metabolites. Glucuronide production was related to 4-HPR concentration as shown in Figure 7, with kinetic parameters provided in Table 3. V_{max} values of 0.62, 2.11 and 0.02 (peak area U·min^{-1}·pmol^{-1} UGT) were determined for UGTs 1A1, 1A3 and 1A6, respectively, with significant differences in V_{max} values observed between all three UGTs. K_m values were high for all UGTs and microsomes investigated, ranging from 389 μM for UGT 1A3 to 1212 μM for HIM.

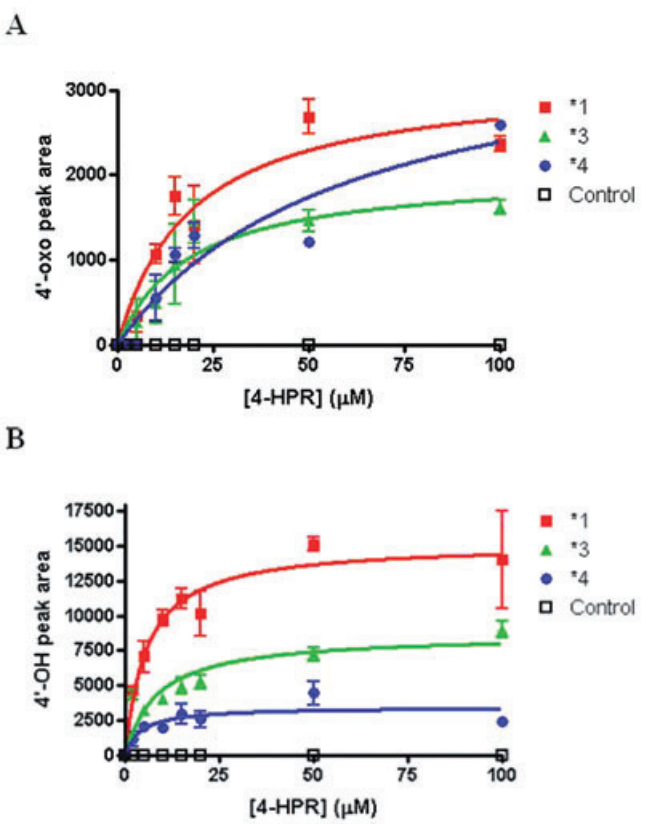

Figure 4

Determination of kinetic parameters for the formation of (A) 4′-oxo fenretinide (4′-oxo 4-HPR) and (B) 4′-OH 4-HPR metabolites by CYP2C8 variants. *E. coli* membrane fractions (0.5 mg·mL^{-1}) co-expressing CYP2C8 variants and P450 reductase were incubated with 0, 2.5, 5, 10, 15 and 20 μM 4-HPR for 3 h. Metabolite formation was determined by high-performance liquid chromatography analysis. Results are mean ± SD from three independent experiments.

Table 2

Determination of kinetic parameters for the formation of the 4′-OH 4-HPR and 4′-oxo 4-HPR metabolites of 4-HPR by CYP2C8 variants

	4′-oxo 4-HPR			4′-OH 4-HPR		
	K_m (μM)	V_{max} (peak area U·min^{-1}·pmol^{-1} CYP)	V_{max}/K_m	K_m (μM)	V_{max} (peak area U·min^{-1}·pmol^{-1} CYP)	V_{max}/K_m
2C8 *1	19.3 ± 5.9	0.04 ± 0.002	0.002	5.6 ± 1.7	0.2 ± 0.007	0.036
2C8 *3	18.8 ± 8.3	0.05 ± 0.001	0.003	8.6 ± 2.5	0.24 ± 0.01	0.028
2C8 *4	59.8 ± 22.5	0.128 ± 0.001	0.002	4.3 ± 2.4	0.11 ± 0.007	0.026

Individual CYP2C8 variants co-expressing P450 reductase, were incubated with 0, 2.5, 5, 10, 15 and 20 μM 4-HPR for 3 h. Metabolite formation was determined by high-performance liquid chromatography analysis. Results are expressed as mean ± SD from $n \geq 3$ experiments. V_{max} for 4′-oxo 4-HPR significantly different for *1 and *4 ($P = 0.0037$) and for *3 and *4 ($P = 0.01$); K_m for 4′-oxo 4-HPR significantly different for *1 and *4 ($P = 0.0035$) and for *3 and *4 ($P = 0.039$); V_{max} for 4′-OH 4-HPR significantly different for *1 and *3 ($P = 0.03$),*1 and *4 ($P = 0.0025$) and for *3 and *4 ($P = 0.0004$).
4-HPR, fenretinide; 4′-OH 4-HPR, 4′-hydroxy fenretinide; 4′-oxo 4-HPR, 4′-oxo fenretinide; CYP, cytochrome P450.

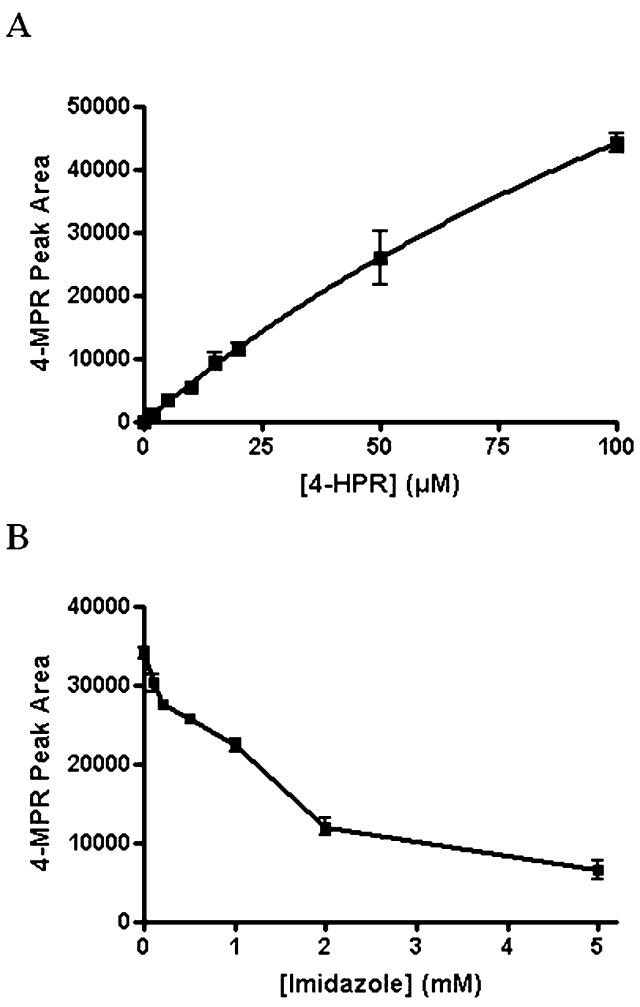

Figure 5

Formation of methoxy fenretinide (4-MPR) following a 3-h incubation of 0.5 mg·mL^{-1} human liver microsomes (HLM) with 0–100 μM fenretinide (4-HPR) and 0.2 mM S-adenosyl methionine (SAM) (A) and following a 3 h incubation of 0.5 mg·mL^{-1} HLM with 50 μM 4-HPR and 0.2 mM SAM in the presence of 0–5 mM imidazole (B).

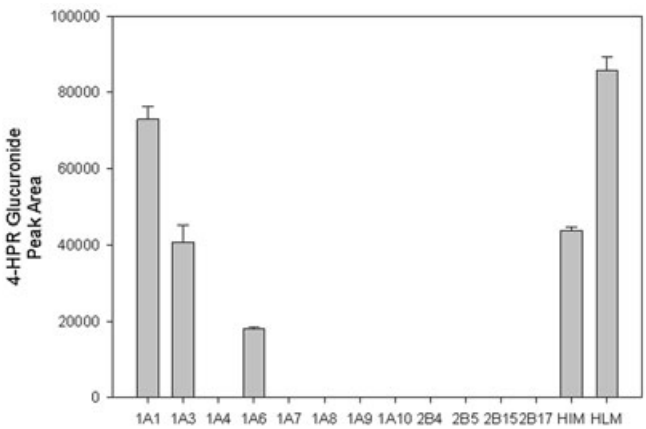

Figure 6

Formation of glucuronide metabolites of fenretinide (4-HPR) by a panel of uridine 5′-diphospho-glucoronosyl transferases (UGT) enzymes, human intestinal microsomes (HIM) and human liver microsomes (HLM). Metabolite formation was determined by HPLC analysis. Metabolites were generated by 3-h incubation of 200 μM 4-HPR with 1 mg·mL^{-1} of each UGT/microsome for 3 h. Results are mean ± SD from three independent experiments.

Discussion and conclusions

The *in vitro* metabolism of 4-HPR was investigated to characterize the key metabolic pathways and the enzymes involved. Elucidation of these enzymes is particularly important as 4-HPR is significantly metabolized *in vivo* to both active and inactive moieties, in the form of 4′-oxo 4-HPR and 4-MPR respectively (Villani *et al.*, 2004; Villablanca *et al.*, 2006; Formelli *et al.*, 2008). We have also identified 4′-OH 4-HPR as an additional polar metabolite of 4-HPR formed *in vitro*. This metabolite is likely to be one of several additional unidentified polar metabolites previously observed by Formelli *et al.* (1989) in breast cancer patients treated with 4-HPR. 4-HPR metabolism is of particular relevance to its clinical utility as the achievement of effective, and consistent plasma concentrations of parent drug in patients has been a key limitation to its clinical development (Maurer *et al.*, 2007).

Initial experiments were carried out to identify the metabolites produced from incubations of 4-HPR with HLM. The individual enzymes responsible for production of these metabolites were then investigated by incubation of 4-HPR with supersomes over-expressing individual human CYP enzymes. The panel of CYPs tested contained those known to be involved in drug metabolism, including CYP3A4, as well as those known to metabolize other retinoids (Marill *et al.*, 2000; 2002; McSorley and Daly, 2000; Zhang *et al.*, 2000). Metabolism to the newly identified metabolite, 4′-OH 4-HPR, was catalysed by all CYPs tested, but to the greatest extent by CYPs 3A4, 3A5 and 2C8. Metabolism to the active metabolite 4′-oxo 4-HPR was only achieved following incubations with CYPs 2C8 and 3A4. This is a similar profile of CYP isoforms to those previously identified as being involved in the metabolism of 9-*cis* retinoic acid, 13-*cis* retinoic acid and ATRA to the corresponding 4-oxo metabolites (Marill *et al.*, 2000; 2002; McSorley and Daly, 2000). It is possible that higher levels of 4-oxo production in HLMs may involve a degree of metabolism not mediated by CYP. Metabolism by CYP2C8 was further investigated, as it is known to be highly polymorphic in the general population (Bahadur *et al.*, 2002) and has previously been shown to play a role in the metabolism of cancer drugs, including paclitaxel (Dai *et al.*, 2001) and other retinoids (Rowbotham *et al.*, 2010b).

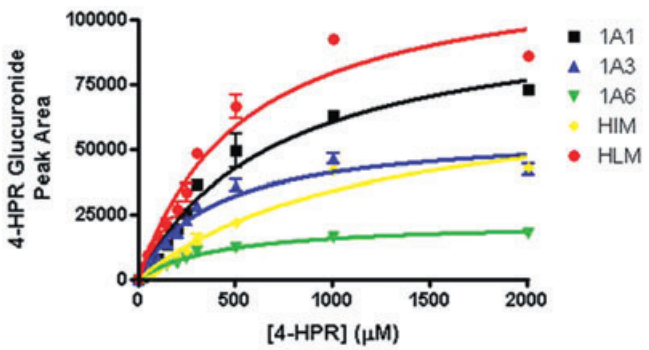

Figure 7

Determination of kinetic parameters for the formation of glucuronide metabolites of fenretinide (4-HPR) by a panel of uridine 5′-diphospho-glucoronosyl transferases (UGT) enzymes, human intestinal microsomes (HIM) and human liver microsomes (HLM); 1 mg·mL^{-1} of the major UGTs found to metabolize 4-HPR (1A1, 1A3 and 1A6, as well as HIM and HLM) were incubated with 0, 5, 25, 50, 75, 100, 150, 200, 250, 300, 500, 1000 and 2000 μM 4-HPR for 3 h. Metabolite formation was determined by high-performance liquid chromatography analysis. Results are mean ± SD from three independent experiments.

Analysis of kinetic parameters of CYP2C8 isoforms demonstrated differences in the metabolism of 4-HPR in terms of metabolism to 4′-oxo 4-HPR and 4′-OH 4-HPR. Most notably, the V_{max} for the formation of 4′-OH 4-HPR was higher for wild-type CYP2C8*1 (V_{max} 0.2 peak area U·min^{-1}·pmol^{-1} CYP) as compared with CYP2C8*4 (V_{max} 0.11 peak area U·min^{-1}·pmol^{-1} CYP), with V_{max}/K_m ratios of 0.028 and 0.026 determined for *3 and *4, respectively, as compared with 0.036 for *1. Conversely, the V_{max} for the formation of 4′-oxo 4-HPR was lower for wild-type CYP2C8*1 (V_{max} 0.04 peak area U·min^{-1}·pmol^{-1} CYP) as compared with CYP2C8*4 (V_{max} 0.128 peak area U·min^{-1}·pmol^{-1} CYP). These data suggest that CYP2C8 genotype may have a considerable impact on the metabolism of 4-HPR, and consequently on the clinical effects of this drug. This pathway of metabolism may be particularly important in tumour cells which are resistant to 4-HPR, but sensitive to the 4′-oxo metabolite (Villani *et al.*, 2006). Of interest, lower activity for CYP2C8*3 and *4, as compared with wild type, has previously been reported *in vitro* for the metabolism of arachidonic acid to epoxyeicosatrienoic acids, with a greater risk of renal toxicity associated with CYP2C8*3 genotype in patients treated with calcineurin inhibitors (Smith *et al.*, 2008). As different expression systems were used, it was not possible to directly compare kinetic parameters obtained

Table 3

Determination of kinetic parameters for the formation of the glucuronide metabolite of 4-HPR by a panel of uridine 5′-diphospho-glucoronosyl transferases (UGT) enzymes, HIM and HLM

	K_m (μM)	V_{max} (peak area U·min^{-1})	V_{max} (peak area U·min^{-1}·pmol^{-1} UGT)
UGT 1A1	716 ± 87	577 ± 34	0.62 ± 0.04
UGT 1A3	389 ± 53	317 ± 18	2.11 ± 0.12
UGT 1A6	422 ± 46	124 ± 6	0.02 ± 0.001
HIM	1212 ± 202	418 ± 38	N/A
HLM	540 ± 69	679 ± 39	N/A

The major UGTs found to metabolize 4-HPR (1A1, 1A3 and 1A6, as well as HIM and HLM) were incubated with 0, 5, 25, 50, 75, 100, 150, 200, 250, 300, 500, 1000 and 2000 μM 4-HPR for 3 h. Metabolite formation was determined by HPLC analysis. Results are expressed as mean ± SD from $n \geq 3$ experiments. V_{max} significantly different for UGT1A1 and UGT1A3 ($P < 0.0001$), for UGT1A1 and UGT1A6 ($P < 0.0001$) and for UGT1A3 and UGT1A6 ($P < 0.0001$); K_m significantly different for UGT1A1 and UGT1A3 ($P = 0.0051$) and for UGT1A1 and UGT1A6 ($P = 0.0066$). Statistical analysis carried out on supersome data only, with V_{max} results standardized to pmol UGT used for analysis.
4-HPR, fenretinide; 4′-OH 4-HPR, 4′-hydroxy fenretinide; 4′-oxo 4-HPR, 4′-oxo fenretinide; CYP, cytochrome P450; HIM, human intestinal microsomes; HLM, human liver microsomes; N/A, no data available.

from CYP2C8 variants expressed in *E. coli* with those obtained from supersomes over-expressing CYP2C8. However, it is reassuring that V_{max}/K_m ratios of comparable magnitude were generated from experiments using the two different approaches.

The effect of known CYP inhibitors was also investigated to further corroborate the involvement of CYPs 3A4 and 2C8 in 4-HPR metabolism. 4-HPR was incubated with HLM in the presence and absence of ketoconazole and/or omeprazole. Ketoconazole considerably inhibited the production of both metabolites, with 75% inhibition of 4′-OH 4-HPR and 85% inhibition of 4′-oxo 4-HPR at 100 μM. Omeprazole alone, at a concentration of 100 μM, had very little effect on either metabolite, but in combination with 100 μM ketoconazole, complete inhibition of both metabolites was observed. No effect was seen with omeprazole in the absence of ketoconazole, as HLM have approximately 25 times more CYP3A4 activity than CYP2C8, meaning that any inhibition of CYP2C8 alone may be masked by the greater activity of CYP3A4 as compared with CYP2C8 in this system. It should be noted that these CYP inhibitors may be relatively non-selective at the concentrations used in these experiments. For example, ketoconazole has been shown to markedly inhibit CYP2C8, as well as CYP3A4, at concentrations >10 μM in a previous study (Ong *et al.*, 2000). Similarly, omeprazole has been shown to inhibit CYPs 2C9 and 2C19 (Li *et al.*, 2004), although the role played by these two enzymes in the metabolism of fenretinide would appear to be minimal. The results obtained in the current study are comparable to the effect of CYP inhibitors on other retinoids; for example, ATRA metabolism has previously been shown to be inhibited approximately 90% by ketoconazole (Schwartz *et al.*, 1995).

In addition to 4′-OH 4-HPR and 4′-oxo 4-HPR, 4-MPR has previously been identified as a major metabolite of 4-HPR (Swanson *et al.*, 1980) and its pharmacokinetic properties have subsequently been investigated (Hultin *et al.*, 1990; Mehta *et al.*, 1998; Vratilova *et al.*, 2004). However, the enzymes responsible for this methylation reaction have not previously been characterized. The identification of SAM as a necessary cofactor for 4-HPR methylation allowed investigations into the formation of all three major 4-HPR metabolites in a single *in vitro* system. Of several candidate methylation enzymes, which require SAM as a cofactor, only a limited number are microsomal. The current study showed that 4-MPR production was not affected by inhibitors of COMT or PMT, but was inhibited up to 80% by imidazole, a competitive substrate for amine-N-methyltransferases, which are known to be microsomal and are involved in the metabolism of many drugs and carcinogens (Ansher and Jakoby, 1986). It was not possible to definitively identify the enzyme involved in this important pathway of 4-HPR metabolism.

Although the formation of 4-HPR glucuronide metabolites has not previously been reported, we investigated the potential for 4-HPR to be metabolized by a panel of recombinant human UGTs as this pathway has previously been shown to be relevant to the metabolism of other retinoid drugs (Czernik *et al.*, 2000; Samokyszyn *et al.*, 2000; Rowbotham *et al.*, 2010a). Although UGTs 1A1, 1A3 and 1A6 were shown to generate 4-HPR glucuronide, it would seem unlikely that this pathway of metabolism will play a significant role in determining 4-HPR disposition in patients.

Retinoids are also known to be significantly metabolized by CYP26, though the contribution of this metabolism cannot be determined by the same methods as for the other CYPs investigated, as supersomes over-expressing CYP26 are not currently available. However, as ATRA is known to induce CYP26 expression, pretreatment of cell lines with ATRA prior to 4-HPR treatment, in conjunction with an assay to determine CYP26 expression would enable investigation into this aspect of 4-HPR metabolism (Armstrong *et al.*, 2005). Once the role played by CYP26 in determining 4-HPR metabolism has been fully ascertained, further ways to modulate this metabolism through the use of retinoic acid metabolism blocking agents may be investigated. Such an approach has already been extensively studied with other retinoids and has been found to consistently reduce retinoid metabolism (Huynh *et al.*, 2006; Njar *et al.*, 2006; Armstrong *et al.*, 2007).

The achievement of effective and consistent plasma concentrations in patients has been a major limitation to the clinical development of 4-HPR. Clinical trials in neuroblastoma patients have shown huge variability in peak plasma concentrations of 4-HPR, varying from 1–20 μM at higher doses (Villablanca *et al.*, 2006). Reformulation of 4-HPR from the currently used oil-based capsules to a lipid matrix has been shown to increase plasma concentrations up to sevenfold in a mouse model (Maurer *et al.*, 2007) and to reduce inter-patient variation in a phase I trial in neuroblastoma patients (Marachelian *et al.*, 2009). Although this largely represents a formulation and bioavailability issue, it is clearly not advantageous for a significant percentage of 4-HPR to be metabolized to inactive metabolites. Indeed, as 4-HPR bioavailability is improved, the level of metabolism to its active, synergistic 4′-oxo 4-HPR metabolite, as compared with the inactive 4-MPR metabolite, may become a more significant factor in determining its overall effectiveness. Identification of the enzymes responsible for 4-HPR metabolism in the current study provides a stepping stone for future studies to determine the potential role of these enzymes in determining the efficacy of 4-HPR.

Acknowledgements

This work was supported by the Medical Research Council (MRC) and Research Councils UK (RCUK).

Conflicts of interest

The authors declare no conflicts of interest.

References

Ansher SS, Jakoby WB (1986). Amine N-methyltransferases from rabbit liver. J Biol Chem 261: 3996–4001.

Armstrong JL, Ruiz M, Boddy AV, Redfern CPF, Pearson ADJ, Veal GJ (2005). Increasing the intracellular availability of all-trans retinoic acid in neuroblastoma cells. Br J Cancer 92: 696–704.

Armstrong JL, Taylor GA, Thomas HD, Boddy AV, Redfern CPF, Veal GJ (2007). Molecular targeting of retinoic acid metabolism in neuroblastoma: the role of the CYP26 inhibitor R116010 in vitro and in vivo. Br J Cancer 96: 1675–1683.

Bahadur N, Leathart JBS, Mutch E, Steimel-Crespi D, Dunn SA, Gilissen R *et al.* (2002). CYP2C8 polymorphisms in Caucasians and their relationship with paclitaxel 6α-hydroxylase activity in human liver microsomes. Biochem Pharmacol 64: 1579–1589.

Czernik PJ, Little JM, Barone GW, Raufman JP, Radominska-Pandya A (2000). Glucuronidation of estrogens and retinoic acid and expression of UDP-glucuronosyltransferase 2B7 in human intestinal mucosa. Drug Metab Dispos 28: 1210–1216.

Dai D, Zeldin DC, Blaisdell JA, Chanas B, Coulter SJ, Ghanayem BI *et al.* (2001). Polymorphisms in human CYP2C8 decrease metabolism of the anticancer drug paclitaxel and arachidonic acid. Pharmacogenetics 11: 597–607.

Formelli F, Carsana R, Costa A, Buranelli F, Campa T, Dossena G (1989). Plasma retinol level reduction by the synthetic retinoid fenretinide: a one year follow-up study of breast cancer patients. Cancer Res 49: 6149–6152.

Formelli F, Clerici M, Campa T, Di Mauro MG, Magni A, Mascotti G *et al.* (1993). Five-year administration of fenretinide: pharmacokinetics and effects on plasma retinol concentrations. J Clin Oncol 11: 2036–2042.

Formelli F, Cavadini E, Luksch R, Garaventa A, Villani MG, Appierto V *et al.* (2008). Pharmacokinetics of oral fenretinide in neuroblastoma patients: indications for optimal dose and dosing schedule also with respect to the active metabolite 4-oxo-fenretinide. Cancer Chemother Pharmacol 62: 655–665.

Garaventa A, Luksch R, Piccolo MSL, Cavadini E, Montaldo PG, Pizzitola MR *et al.* (2003). Phase I trial and pharmacokinetics of fenretinide in children with neuroblastoma. Clin Cancer Res 9: 2032–2039.

Gatta G, Capocaccia R, Coleman MP, Gloeckler LA, Berrino F (2002). Childhood cancer survival in Europe and the United States. Cancer 95: 1767–1772.

Hultin TA, Filla MS, McCormick DL (1990). Distribution and metabolism of the retinoid N-(4-Methoxyphenyl)-all-trans-retinamide, the major metabolite of N-(4-Hydroxyphenyl)-all-trans-Retinamide, in female mice. Drug Metab Dispos 18: 175–179.

Huynh CK, Brodie AMH, Njar VCO (2006). Inhibitory effects of retinoic acid metabolism blocking agents (RAMBAs) on the growth of human prostate cancer cells and LNCaP prostate tumour xenografts in SCID mice. Br J Cancer 94: 513–523.

Kitareewan S, Spinella MJ, Allopenna J, Reczek PR, Dmitrovsky E (1999). 4HPR triggers apoptosis but not differentiation in retinoid sensitive and resistant human embryonal carcinoma cells through an RAR independent pathway. Oncogene 18: 5747–5755.

Li X-Q, Andersson TB, Ahlström M, Weidolf L (2004). Comparison of inhibitory effects of the proton pump-inhibiting drugs omeprazole, esomeprazole, lansoprazole, pantoprazole, and rabeprazole on human cytochrome P450 activities. Drug Metab Dispos 32: 821–827.

Lovat PE, Ranalli M, Annichiarrico-Petruzzelli M, Bernassola F, Piacentini M, Malcolm AJ *et al.* (2000). Effector mechanisms of fenretinide-induced apoptosis in neuroblastoma. Exp Cell Res 260: 50–60.

McSorley LC, Daly AK (2000). Identification of human cytochrome P450 isoforms that contribute to all-trans-retinoic acid 4-hydroxylation. Biochem Pharmacol 60: 517–526.

Marachelian A, Kang MH, Hwang K, Villablanca JG, Groshen S, Matthay KK *et al.* (2009). Phase I study of fenretinide (4-HPR) oral powder in patients with recurrent or resistant neuroblastoma: New Approaches to Neuroblastoma Therapy (NANT) Consortium trial. J Clin Oncol 27 (15S): 10009.

Marill J, Cresteil T, Lanotte M, Chabot G (2000). Identification of human cytochrome P450s involved in the formation of all-trans-retinoic acid principal metabolites. Mol Pharmacol 58: 1341–1348.

Marill J, Capron CC, Idres N, Chabot GG (2002). Human cytochrome P450s involved in the metabolism of 9-cis- and 13-cis-retinoic acids. Biochem Pharmacol 63: 933–943.

Maurer BJ, Kalous O, Yesair DW, Wu X, Janeba J, Maldonado V *et al.* (2007). Improved oral delivery of N-(4-hydroxyphenyl) retinamide with a Novel LYM-X-SORB organized lipid complex. Clin Cancer Res 13: 3079–3086.

Mehta RR, Hawthorne ME, Graves JM, Mehta RG (1998). Metabolism of N-[4-hydroxyphenyl]retinamide (4-HPR) to N-[4-methoxyphenyl]retinamide (4-MPR) may serve as a biomarker for its efficacy against human breast cancer and melanoma cells. Eur J Cancer 34: 902–907.

Myatt SS, Burchill SA (2007). The sensitivity of the Ewing's sarcoma family of tumours to fenretinide-induced cell death is increased by EWS-Fli1-dependent modulation of p38MAPK activity. Oncogene 27: 985–986.

Njar VCO, Gediya L, Purushottamachar P, Chopra P, Vasaitis TS, Khandelwal A *et al.* (2006). Retinoic acid metabolism blocking agents (RAMBAs) for treatment of cancer and dermatological diseases. Bioorg Med Chem 14: 4323–4340.

Ong C-E, Coulter S, Birkett DJ, Bhasker CR, Miners JO (2000). The xenobiotic inhibitor profile of cytochrome P4502C8. Br J Clin Pharmacol 50: 573–580.

Ponthan F, Lindskog M, Karnehed N, Castro J, Kogner P (2003). Evaluation of anti-tumour effects of oral fenretinide (4-HPR) in rats with human neuroblastoma xenografts. Oncol Rep 10: 1587–1592.

Rowbotham SE, Illingworth NA, Daly AK, Veal GJ, Boddy AV (2010a). Role of UDP-glucuronosyltransferase isoforms in 13-cis retinoic acid metabolism in humans. Drug Metab Dispos 38: 1211–1217.

Rowbotham SE, Boddy AV, Redfern CPF, Veal GJ, Daly AK (2010b). Relevance of non-synonymous CYP2C8 polymorphisms to 13-cis retinoic acid and paclitaxel hydroxylation. Drug Metab Dispos 38: 1261–1266.

Samokyszyn VM, Gall WE, Zawada G, Freyaldenhoven MA, Chen G, Mackenzie PI *et al.* (2000). 4-hydroxyretinoic acid, a novel substrate for human liver microsomal UDP-glucuronosyltransferase(s) and recombinant UGT2B7. J Biol Chem 275: 6908–6914.

Schwartz EL, Hallam S, Gallagher RE, Wiernik PH (1995). Inhibition of all-trans-retinoic acid metabolism by fluconazole in vitro and in patients with acute promyelocytic leukemia. Biochem Pharmacol 50: 923–928.

Smith HE, Jones JP, Kalhorn TF, Farin FM, Stapleton PL, Davis CL *et al.* (2008). Role of cytochrome P450 2C8 and 2J2 genotypes in calcineurin inhibitor-induced chronic kidney disease. Pharmacogenet Genomics 18: 943–953.

Swanson BN, Zaharevitz DW, Sporn MB (1980). Pharmacokinetics of N-(4-hydroxyphenyl)-all-trans-retinamide in rats. Drug Metab Dispos 8: 168–172.

Villablanca JG, Krailo MD, Ames MM, Reid JM, Reaman GH, Reynolds CP (2006). Phase I trial of oral fenretinide in children with high-risk solid tumors: a report from the Children's Oncology Group (CCG 09709). J Clin Oncol 24: 3423–3430.

Villani MG, Appierto V, Cavadini E, Valsecchi M, Sonnino S, Curley RW *et al*. (2004). Identification of the fenretinide metabolite 4-oxo-fenretinide present in human plasma and formed in human ovarian carcinoma cells through induction of cytochrome P450 26A1. Clin Cancer Res 10: 6265–6275.

Villani MG, Appierto V, Cavadini E, Bettiga A, Prinetti A, Clagett-Dame M *et al*. (2006). 4-oxo-fenretinide, a recently identified fenretinide metabolite, induces marked G2-M cell cycle arrest and apoptosis in fenretinide-sensitive and fenretinide-resistant cell lines. Cancer Res 66: 3238–3247.

Vratilova J, Frgala T, Maurer BJ, Reynolds PC (2004). Liquid chromatography method for quantifying N-(4-hydroxyphenyl)retinamide and N-(4-methoxyphenyl)retinamide in tissues. J Chrom B 808: 125–130.

Zhang Q, Dunbar D, Kaminsky L (2000). Human cytochrome P-450 metabolism of retinals to retinoic acids. Drug Metab Dispos 28: 292–297.